THE ASTROPHYSICAL JOURNAL, 565:244–255, 2002 January 20
© 2002. The American Astronomical Society. All rights reserved. Printed in U.S.A.

X-RAY EMISSION PROCESSES IN RADIO JETS

D. E. HARRIS
Smithsonian Astrophysical Observatory, 60 Garden Street, Cambridge, MA 02138; harris@cfa.harvard.edu
AND
H. KRAWCZYNSKI
Yale University, P.O. Box 208101, New Haven, CT 06520-8101; krawcz@astro.yale.edu
Received 2001 July 26; accepted 2001 September 25

ABSTRACT

The emission processes responsible for the observed X-rays from radio jets are commonly believed to be nonthermal, but in any particular case, it is unclear if synchrotron emission or one or more varieties of inverse Compton emission predominates. We present a formulation of inverse Compton emission from a relativistically moving jet ("IC/beaming") that relies on radio-emitting synchrotron sources for which the energy densities in particles and fields are comparable. We include the nonisotropic nature of inverse Compton scattering of the relativistic electrons on photons of the cosmic microwave background (CMB) and provide beaming parameters for a number of jets. A list of X-ray–emitting jets is given and the jets are classified on the basis of their morphology and spectral energy distribution to determine their likely emission process. We conclude that these jets have significant bulk relativistic velocities on kiloparsec scales, that higher redshift sources require less beaming because the energy density of the CMB is significantly greater than locally, and that for some nearby sources synchrotron X-ray emission predominates because the jet makes a large angle to the line of sight.

Subject headings: galaxies: jets — magnetic fields — radiation mechanisms: nonthermal

1. INTRODUCTION

X-ray emission associated with radio jets in extragalactic sources now comes in a large variety of diverse characteristics. When this sort of emission was first isolated (e.g., the radio galaxy M87 with the *Einstein Observatory*; Schreier, Gorenstein, & Feigelson 1982) and there were only a few examples, it was tempting to work on the assumption that the emission process was definable and would apply to all examples. This notion persisted into the *ROSAT* era until a convincing case was made that the terminal hot spots of Cygnus A represented synchrotron self-Compton (SSC) emission (Harris, Carilli, & Perley 1994).

With the advent of the *Chandra Observatory*, the number of sources has almost tripled (from seven to at least 19), yet there remain substantial problems in determining the emission process responsible for the X-rays in some sources. Although broken power laws connecting the radio, optical, and X-ray data are still viable spectral models for a few sources, a number of other sources are observed to have such a low flux density in the optical that the indicated cutoff in the spectrum would preclude a simple connection to the X-ray data.

The introduction of the "beaming model" (Tavecchio et al. 2000; Celotti, Ghisellini, & Chiaberge 2001) in the particular case of PKS 0637 was presented as an escape from this dilemma. In this model, the enhancement of the X-ray emission relative to the synchrotron (radio/optical) is explained by hypothesizing a bulk velocity of the jet fluid that is relativistic even on large (kiloparsec) scales. If this were the case, in the frame of the jet the effective photon energy density of the cosmic microwave background (CMB) would be augmented by the square of the jet's Lorentz factor, Γ, and it was demonstrated that quite reasonable combinations of Γ and the beaming factor, δ, could be invoked to explain the observed intensities.

In this paper we review the common emission processes (§ 2), present a current list of jet sources and suggest a classification scheme (§ 3), describe a formulation of the beaming model that relies on an evaluation of the magnetic field strength from the equipartition field and includes the anisotropic nature of the inverse Compton (IC) scattering (§ 4), and examine the conflicting evidence and ramifications for the synchrotron and IC models (§ 5). Appendices A and B contain the details of our beaming formulation.

For numerical results we use cgs units unless stated otherwise and assume $H_0 = 50$ km s^{-1} Mpc^{-1} and $q_0 = 0$. We follow the convention that the spectral index of a power law is defined by flux density, $S_\nu = k\nu^{-\alpha}$.

2. OVERVIEW OF EMISSION PROCESSES

2.1. *Thermal Bremsstrahlung*

For many sources that display convincing evidence that the X-ray and radio emission originate in the same volume (e.g., hot spot B of 3C 390.3; Harris, Leighly, & Leahy 1998), it has been argued that thermal bremsstrahlung does not provide a satisfactory model for the X-ray emission because the required amount of hot gas is large ($\approx 10^{10}\ M_\odot$), overpressured, and far from the parent galaxy and the predicted Faraday rotation and depolarization are not observed. Recent *Chandra* results (e.g., 3C 273; Marshall et al. 2001a) confirm that the X-ray emission from jet features has no line emission and is best characterized by a power law.

2.2. *Synchrotron Emission*

Synchrotron emission has been considered the "process of choice" for X-rays from knots in radio jets mainly because the optical polarization observed in sources such as M87 is convincing evidence that the optical emission as well as the radio emission comes from the synchrotron process. Demonstrations that the X-ray intensity was consistent either with a single power-law extrapolation from radio and optical bands (e.g., hot spot B of 3C 390.3; Harris et al. 1998) or with a broken power law (e.g., knot A in M87; Biretta, Stern, & Harris 1991) were taken as circumstantial

evidence that the X-rays were also generated by synchrotron emission. Required for this model is the presence of electrons with Lorentz factor $\gamma > 10^7$ (compared to values of 10^5 for optical emission). In the typical equipartition fields of $B \approx 10^{-4}$ G, the radiation half-lives τ_0 of the X-ray–emitting electrons would be of order 10 yr (however, see Aharonian 2001 for problems associated with very fast cooling times).

There are, however, a number of sources for which the optical flux densities or limits preclude a simple construction of a broken power law. In general, assuming the usual shock acceleration processes and dominance of losses to the relativistic electrons that go with the energy squared, we expect that both the electron distribution and the resulting synchrotron emission spectrum will be concave downward when displayed on the usual log S_ν versus log ν plot. For this reason, X-ray intensities that lie well above the extrapolation of the radio/optical synchrotron spectrum are taken to be strong evidence against the "simple" synchrotron model.

The emission of most of these sources, however, can still be explained with inhomogeneous synchrotron models. Spatially separated emission components that cannot be resolved with the current X-ray detectors would be the consequence of diffusive shock acceleration with a time-dependent high energy cutoff of accelerated particles. While the low-energy radio and optical emission is dominated by radiatively aged particle populations further downstream, the X-ray emission is emitted only by recently accelerated particles. In this scenario the projected extension of the X-ray emission region is given either by the projected size of the accelerating shock or by the distance the downstream plasma travels before the highest energy electrons cool away. For 3C 120, such an interpretation encounters the difficulty that the optical to X-ray energy spectrum is as hard as $\alpha_{OX} < 0.35$, which indicates a spectrum of accelerated particles with a spectral index $p \leq 1.7$ (even in the optimistic case that the X-ray electrons did not cool substantially)—harder than the canonical value of 2 expected for acceleration at strong nonrelativistic shocks.

Another class of models involves high-energy protons. These models and their difficulties are described in Mannheim, Krulls, & Biermann (1991) and Aharonian (2001).

2.3. *Inverse Compton Emission*

Inverse Compton emission has a distinct advantage over X-ray synchrotron emission in that extremely high energies for the emitting electrons are not required. What is required are both enough electrons and enough energy density in photons of the proper energy to produce the desired scattered photons: $\nu_{out} \approx \nu_{in} \times \gamma^2$.

2.3.1. *Synchrotron Self-Compton Emission*

Unlike synchrotron emission for which the radio data often provide no clear indication about the higher energy parts of the electron spectrum, accurate predictions of source intensity can be calculated for SSC emission. Given a reasonable estimate for the emitting volume, it is possible to calculate the photon energy density from the synchrotron spectrum and then determine what B-field is required to have the right number of electrons to give the observed (radio) synchrotron and the observed (X-ray) IC emissions.

Although SSC emission is mandatory for all synchrotron sources, it is usually the case that the photon energy density (u_ν) is significantly smaller (i.e., by factors of 100 or more) than the energy density of the magnetic field (u_B), and thus the major energy loss for all electrons is via synchrotron emission (and the SSC component is too weak to observe or distinguish from other emissions).

There are, however, four FR II radio galaxies with convincing SSC X-ray emission from their (terminal) hot spots: Cyg A (Harris et al. 1994; Wilson, Young, & Shopbell 2000); 3C 295 (Harris et al. 2000); 3C 123 (Hardcastle, Birkinshaw, & Worrall 2001a), and 3C 263 (M. J. Hardcastle et al. 2002, in preparation). For all of these sources, predicted SSC emission was calculated from the radio data, proposals were written, and the hot spots were detected as predicted. In all cases, the average magnetic field strengths derived from the SSC equations are consistent with equipartition fields for the case of little or no contribution to the particle energy density from relativistic protons. The hot spots of these sources are, so far, the only resolved structures for which convincing SSC models have been published.

2.3.2. *IC Emission from the Microwave Background*

Except for high-redshift sources, IC emission from the relativistic electrons scattering off the CMB is incapable of producing the observed intensity of X-rays unless the beaming model is invoked with relativistic values of the bulk jet velocity (see § 4). The beaming model is attractive because most or all of the X-ray–emitting jets are one sided and the model permits the relative increase of the effective photon energy density to that in the magnetic field, thereby boosting the emission in the IC channel relative to that in the synchrotron channel.

2.3.3. *IC Emission from other Photons*

External photons have been employed successfully in explaining X-ray emission from some radio lobes (Brunetti et al. 2001). However, it is unlikely to apply to knots far removed from the hypothesized highly luminous quasar-like core, and Brunetti's model provides IC enhancement on the receding side of the source, not the approaching side, as observed in our sample.

Celotti et al. (2001) discuss the possibility that emission from a high velocity "spine" of a jet may serve as seed photons for IC emission from a lower velocity sheath. Generally, a wide latitude of inventiveness is allowed for IC emission since the dominant contribution to the photon energy density may be anisotropic and hence not directly observable.

3. CLASSIFICATION OF SOURCES

The contents of this section are subject to change since much of our information is incomplete. The reason for including this source list is to provide an overview. Some aspects of the classification are subjective, and we anticipate changes as new data become available.[1]

Table 1 contains a list of bona fide X-ray jet sources known to us as of 2001 March. In the last column is the classification which is described here.

3.1. *SSC*

This category is perhaps more secure than the others because the data confirm the predictions rather well. All four SSC sources (§ 2.3.1) are FR II radio galaxies, and their

[1] We maintain current information at http://hea-www.harvard.edu/XJET/.

TABLE 1

2001 March List of Radio Sources with Jet-related X-Ray Emission

Generic Name	R.A. (J000.0)	Decl. (J000.0)	z	Distance ($H = 50$) (Mpc)	kpc/arcsec ($H = 50$)	Associated Radio	Associated Optical	P.A. with Respect to Core	Classification
3C 15	00 37	−01 09	0.0730	453	1.91	Knots	Knots	−30	Nyc
3C 31	01 07	32 25	0.0167	101	0.47	Jet	No	−20	Nyc
3C 66B.....	02 23	43 00	0.0215	130	0.61	Jet	Jet	45	Sync
3C 120	04 33	05 21	0.0330	201	0.91	Knot	No	NW	Beam?
3C 123	04 37	29 40	0.2177	1448	4.74	HS	No	110	SSC
Pictor A	05 19	−45 46	0.0350	214	0.97	W HS	Yes	−80	Beam
PKS 0521 ...	05 25	−36 27	0.055	338	1.475	Knots	Yes	NW	Nyc
PKS 0637 ...	06 35	−75 16	0.653	5197	9.22	Knots	Yes	−90	Beam
PKS 1127 ...	11 30	−14 49	1.18	11257	11.48	Yes	?	42	Dis.morph.
3C 263	11 39	65 47	0.6563	5230	9.25	Yes	No?	116	SSC
3C 273	12 29	02 02	0.1583	1025	3.70	Knots	Knots	190	Sync, Beam
NGC 4261...	12 19	05 49	0.00737	44	0.21	Yes	No?	−90	Nyc
M87	12 30	12 23	0.00427	16	0.077	Knots	Knots	−60	Sync
Cen A	13 26	−42 49	...	3.5	0.017	?	?	70	Dis.morph.
3C 295	14 11	52 13	0.45	3307	7.63	2 HS	Yes	−10	SSC
3C 371	18 06	69 49	0.051	314	1.38	Yes	Yes	WSW	Sync
3C 390.3	18 42	79 46	0.0561	346	1.50	HS B	HS B	−10	Sync
Cyg A	19 59	40 44	0.0560	345	1.50	2 HS	No	110/280	SSC

Notes.—Units of right ascension are hours and minutes, and units of declination are degrees and arcminutes.We assume $q_0 = 0$. References for individual sources as well as contact persons for unpublished data can be found at the XJET Web site (see footnote 1). In the classification column, "Nyc" means "not yet classified" (the data are unpublished), and "Dis.morph." signifies "discrepant morphology." Morphology: We generally use "knot" to indicate a distinct brighter feature in a jet that continues past the feature, and "hot spot" ("HS") either as the terminal bright enhancement at the end of an FR II jet or as one of the multiple features associated with the termination of a jet. Normally, knots are found on the inner portion of FR I jets, whereas hot spots are mostly at the ends of FR II jets. However, we are not trying to impose distinct definitions and infer no physical differences beyond these generalities.

terminal hot spots rather than brightness enhancements in the jets are the SSC emitters. For all of these, the magnetic field strengths in the hot spots are in the range 100–400 μG, values consistent with the equipartition field for the case of little or no contribution to the particle energy density from protons. Synchrotron luminosities and lifetimes are unaffected by the IC losses, and the electrons responsible for the observed X-rays are those emitting synchrotron emission in the normal radio band. Alternative models for these hot spots are the generation of high-energy electrons via the PIC (proton-induced cascade; Mannheim et al. 1991) or proton synchrotron (Aharonian 2001) processes, both of which would require much stronger magnetic fields ($B \gg 500$ μG).

3.2. *Synchrotron*

Mindful of ongoing debate about the evidence for spectral cutoffs from optical data (§ 2.2), we classify M87 knots D, A, and B as synchrotron emitters (Biretta et al. 1991; Marshall et al. 2001b). Additional sources in this category are 3C 390.3 hot spot B (Harris et al. 1998), knots A1 and B1 in the 3C 273 jet (Marshall et al. 2001a), and 3C 66B (Hardcastle, Birkinshaw, & Worrall 2001b), although for some of these, there is the problem that a cooling break in the emission spectrum has not been isolated.

The extension of the synchrotron spectrum from the optical to the X-ray has only a small effect on the total energy and on the calculation of the equipartition magnetic field. However, this model requires the extension of the electron spectrum from $\gamma \approx 10^5$ to $\geq 10^7$. The primary observable consequence is that the electrons responsible for the X-rays have lifetimes of order 10–100 yr.

If a somewhat ad hoc additional spectral component is allowed (§ 5.2; i.e., a high-energy component of the electron energy distribution with a flatter spectrum than that observed in the radio/optical domain), then synchrotron emission models can be devised for sources such as Pictor A (Wilson, Young, & Shopbell 2001, § 4.2.2.2), 3C 273 knot D, PKS 0637, and 3C 120 (Harris et al. 1999; where a very hard spectral index of accelerated particles of $p = 1.7$ would be required). The SSC sources (§ 2.3.1) could also be accommodated by synchrotron models if additional spectral components are allowed.

3.3. *Bulk Relativistic Velocities*

In §§ 4 and 5 we discuss many of the details and ramifications of this model. While there is little debate concerning the utility of the beaming model in its ability to explain a larger ratio of X-ray to synchrotron emission than other models, there is no completely convincing evidence that kiloparsec-scale jets actually have bulk velocities close to c.

Beaming models have been presented for PKS 0637 (Celotti et al. 2001; Tavecchio et al. 2000) and for 3C 273 (Sambruna et al. 2001). For the knots in these jets, viewing angles are generally required to be less than 10°, Γ-values range from 5 to 20, and equipartition fields are significantly smaller than for unbeamed synchrotron emission. A very significant difference between beaming and synchrotron models is that the beaming model posits that the electrons responsible for the observed X-rays are at the very bottom of the electron distribution, with γ in the range 20–150. This implies that no variability is expected in the X-ray intensity. Because there is a significant difference between the electron energies producing the X-rays and those that produce radio synchrotron emission observable from the Earth with sufficient resolution to measure accurate spectral indices, there is a large uncertainty in the expected spectral shape of the electron distribution at low energies and, consequently, in

the predicted spectral shape and the intensity of the X-ray emission.

3.4. *Discrepant Radio/X-Ray Morphologies*

Although most of the sources in Table 1 display spatial coincidence between the radio, X-ray, and optical morphologies, there are a few sources where this is not the case. Cen A, 3C 66B, and PKS 1127 are the three examples of this behavior in our collection. We do not believe that this effect results from limited angular resolution since it occurs in both the nearest (Cen A) and furthest (PKS 1127) source. In the case of Cen A (Kraft et al. 2000), some offsets between the peak brightness of radio and X-ray are of order 2″ (34 pc), while other features are coincident. For PKS 1127, an offset of 0.″8 observed for knot B corresponds to 9 kpc.

For these jets, it is difficult to measure radio and X-ray intensities for well-defined volumes. It is also the case that the PKS 1127 jet is very weak in the radio (the source is a Very Large Array calibrator), and the published radio data for Cen A do not have the combination of high resolution and signal-to-noise ratio that are necessary for reliable interband comparisons. For 3C 66B and PKS 1127, the peak X-ray brightness occurs upstream of the peak radio brightness. To obtain significant X-ray emission with little or no radio emission would require extreme beaming parameters or a distinct low-energy electron population (§ 5.2) for the beaming model or a flat high-energy component of the electron spectrum for synchrotron models.

3.5. *Not Yet Classified*

Since data have not yet been published, we have not classified 3C 15, 3C 31, PKS 0521, and NGC 4261 in Table 1.

4. DETERMINATION OF JET PARAMETERS WITHIN THE BEAMING MODEL

The beaming model introduced by Tavecchio et al. (2000) and Celotti et al. (2001) is appealing because it offers a method of increasing the IC emission relative to the synchrotron emission and because it was already clear from *Einstein* and *ROSAT* results on M87, 3C 120, and 3C 390.3 that all known X-ray–emitting jet features were one sided. Most of the new examples from *Chandra* detections maintain the one-sided nature of X-ray emission, a natural consequence of the beaming model.

The following formulation is based on the assumption of equipartition in the synchrotron source in order to evaluate the magnetic field strength and accounts for the anisotropic nature of the IC emission in the jet frame. The details are given in Appendix A.

We define the constraints on the bulk relativistic flow velocity of the jet fluid, Γ, the viewing angle of the line of sight of the observer with respect to the jet velocity vector, θ_j, and the relativistic Doppler factor, δ. Once these constraints have been evaluated, we examine a number of source parameters:

1. the segments of the electron energy spectrum responsible for both the synchrotron and IC emissions to make sure we end up with a self-consistent source model,
2. the half-lives of the various energy electrons, and
3. the basic parameters of the synchrotron source in the jet frame.

4.1. *The Case for Equipartition*

Over the years since its introduction (Burbidge 1956), the concept of "minimum energy" (or "equipartition") has generated considerable debate and some confusion. Our view is that although it was originally borne of twin desperations (the staggering amount of nonthermal energy required for large synchrotron radio sources and the realization that it was almost impossible to disentangle the two primary parameters of synchrotron emission), a reasonable case can be advanced that most extragalactic synchrotron sources are not more than a factor of a few from having their average magnetic field energy density equal to the average energy density in relativistic particles: $u(p) \approx u(B)$.

Obviously, we are unconcerned with the condition $u(p) \ll u(B)$; it is the converse that has generated some interest as a means of increasing the relative emission in the IC channel compared to that in the synchrotron channel. For radio structures far from their parent galaxy, it seems that the only mechanism that serves to maintain the integrity of a radio lobe is the magnetic field, acting as a boundary between the nonthermal plasma and the external thermal plasma. Direct evidence that some synchrotron-emitting plasmas maintain their identity is provided both by the detection of cavities in cluster gas (Carilli, Perley, & Harris 1994) and by the observation that the B-field direction is normally tangent to the edges of radio lobes (and not tangled, as expected if turbulent mixing were occurring). If the particle energy density were much greater than $u(B)$, it is unlikely that the field would confine the particles, and radio sources would be transient phenomena without well-defined boundaries.

Evidence for equipartition has come from the analyses of X-ray emission from terminal hot spots. In the study of Cygnus A hot spots, Harris et al. (1994) argued that if the observed X-ray emission were to be SSC emission, then the average magnetic field strengths ($B_{\rm IC}$) would be very close to the equipartition fields estimated from the conditions: filling factor = 1 and no contribution to the particle energy density from relativistic protons. Since we have a fairly accurate estimate of the synchrotron photon energy density, we know that if there were more electrons than those corresponding to $B_{\rm eq}$, we would overproduce the X-ray emission. Thus, the derived value of $B_{\rm IC}$ is a firm lower limit, and the only method of driving the hot spots out of equipartition with $u(p) \gg u(B)$ would be to add nonradiating particles. The three recent additions to the collection of resolved SSC emitters strengthen this evidence.

A number of additional arguments have been presented in favor of synchrotron sources being close to equipartition. Readhead (1994) used the observed distribution of brightness temperatures in support of equipartition but did not deal with the physical mechanism responsible. Bodo, Ghisellini, & Trussoni (1992) refined earlier work by Ginzburg & Syrovatskii (1969) and Singal (1986) on the effects of spiraling electrons and their associated diamagnetic moments and stated, "The counterfield produced by a cloud of relativistic electrons leads to an equilibrium between the magnetic field in the cloud and the energy density of radiating electrons."

Although it is possible to imagine synchrotron sources shortly after the introduction of a large amount of energy in particles, it is beyond the scope of this paper to consider the timescale required to return to equipartition. Since we are

TABLE 2

BEAMING PARAMETERS FOR SELECTED JET FEATURES

		INPUT PARAMETERS				BEAMING PARAMETERS			JET LENGTH			JET FRAME SYNCHROTRON PARAMETERS			HALF-LIFE OBSERVED AT EARTH	
SOURCE	KNOT	z	α	$B(1)$ (μG)	$R(1)$	Γ δ	θ (deg)	R'	DfC (arcsec)	Proj. (kpc)	Phys. (kpc)	γ Range (Synchrotron)	γ Range (0.3–8 keV)	B'(eq) (μG)	ν_s(max) (Hz)	$\tau[\nu_s(\max)]$ (yr)
M87	HST-1	0.00267	0.71	272	0.264	40	1.2	551	1	0.08	4	30–9.4E5	12– 61	7	1E15	4.0
	D	...	0.70	319	0.0568	33	1.8	123	3	0.23	7	22–8.7E5	20–107	10	1E15	7.7
	A	...	0.67	288	0.006	19	2.8	21	12	0.92	19	29–9.1E5	34–174	15	1E15	38.
	B	...	0.67	248	0.0013	11	4.7	3	15	1.15	14	31–9.8E5	56–290	22	1E15	168.
3C 120	25″	0.033	0.54	41	0.04	39	1.5	15764	25	23	869	77–2.4E4	17–89	1.1	1E11	153.
3C 273	A1	0.158	0.79	172	1.09	25	2.3	246	13	48	1196	40–1.3E6	27–139	6.9	1E15	7.6
	B1	...	0.85	134	3.5573	20	2.8	166	17	62	1269	45–1.4E6	34–174	6.7	1E15	13.8
	D/H	...	0.57	221	0.00017	10	5.5	5	20	75	783	35–1.1E6	67–348	22	1E15	132.
PKS 0637...	wk7.8	0.651	0.81	195	0.209	9.9	5.7	21	8	72	725	45–1.4E6	68–351	20	1E15	39.
PKS 1127...	Inner	1.187	1.0	144	8.426	5.2	11	8	1.5	17	89	60–1.9E4	130– 669	28	1E11	8348.
	Rect.	...	1.33	24	8.9E4	2.9	20	31	11	126	368	147–4.6E4	232–1200	8.3	1E11	20300.
	A	...	0.76	13	0.667	3.7	15	287	12	138	533	200–6.3E4	182– 940	3.5	1E11	7195.
	B	...	0.92	29	1.106	2.2	26	7	19	221	504	134–4.2E4	306–1580	13.2	1E11	49500.
	C	...	0.94	29	0.754	1.5	32	3	28	321	606	134–4.2E4	449–2318	19	1E11	138700.

NOTES.—Length: "DfC" is distance from the core in arcseconds, projected kiloparsecs, and deprojected kiloparsecs (= projected/sin θ) for no bending. The γ range for the radio (synchrotron spectrum) corresponds to the frequency range of 1 MHz to the value of ν_s(max) given in a later column. The synchrotron spectrum is assumed to extend down to 1 MHz in order to include the low-energy electrons required for the beaming model. The term ν_s(max) is the highest reliable synchrotron frequency: radio (E11 Hz) or optical (E15 Hz). The term τ is the half-life for electrons that produce ν_s(max). The term R' is the ratio of IC to synchrotron losses in the jet frame. The column "θ" gives the maximum value of the angle between the line of sight and the jet axis for which there are valid solutions; at this angle, $\Gamma = \delta$.

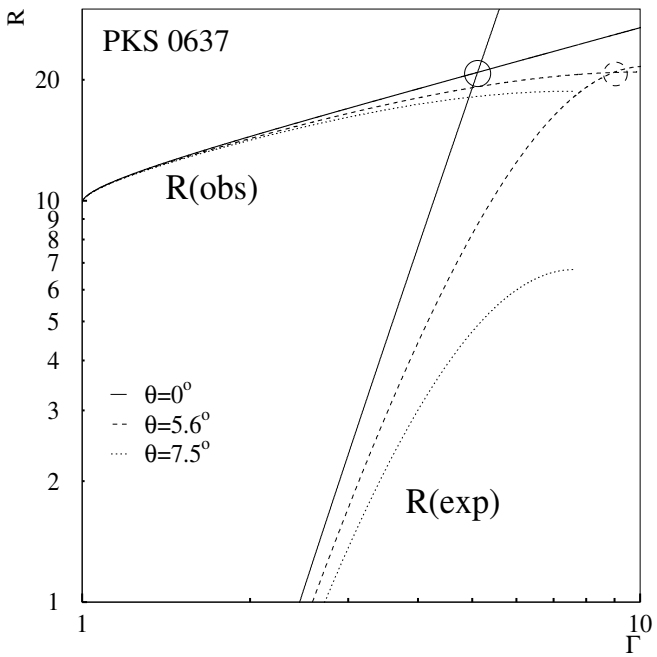

FIG. 1.—Illustration of the solutions for eqs. (A21) and (A22). The vertical axis is the ratio of IC to synchrotron losses in the jet frame, and the horizontal axis is the Lorentz factor for the bulk velocity of the jet fluid. For PKS 0637, the range of solutions runs from $\theta = 0°$ to 5°.6. For larger values of θ, there is no solution.

dealing with large (>kpc) scale structures, we believe that most of the emitting regions considered in this paper will be close to equipartition. However, questions are often raised such as, "What is the extent of departure from equipartition

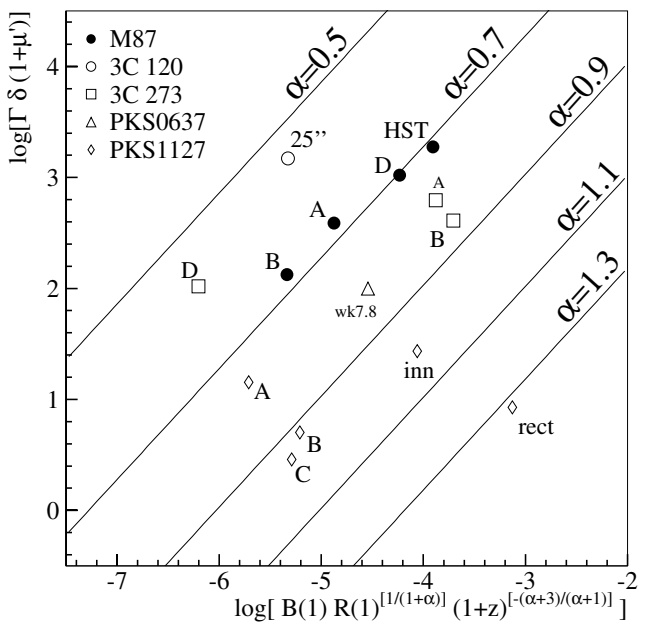

FIG. 2.—Graphic illustration of eq. (A24). Since the second Γ term of eq. (A23) has been dropped, the results shown here are indicative only. Solutions for several values of the spectral index are shown by the solid lines. The source data from Table 2 demonstrate that steeper spectra and higher redshifts require less beaming than do lower redshift, flatter spectra knots. Of the four observables contributing to the *x*-axis value, the equipartition field for no beaming, $B(1)$, varies by a factor of 10, whereas $R(1)$ varies by at least 9 orders of magnitude (mitigated here, of course, by the exponent, which is usually less than unity).

for some given condition?" We note from equation (A24) that a given change in Γ (which involves the same change in δ) will require a change in $B(1)$ by this factor squared, and since $u(B)$ goes as B^2, the change to $u(B)$ goes as the fourth power. As an example, consider the beaming required for 3C 120: $\Gamma = 39$ (Table 2). How far from equipartition would we have to go to get $\Gamma = 10$? The answer is, of order 230 times less energy in the magnetic field than in particles. Although this calculation is approximate, the formulation presented in Appendices A and B relies on the equipartition assumption only to evaluate the average field strength, and if some other estimate is available, it can be used in place of B'_{eq} in equation (A23).

4.2. *Outline of the Method*

We first take the synchrotron spectrum from the observer's frame back to the jet frame. Since the beaming factor is unknown, this process is done (in principle) for trial values of δ. In the jet frame, we apply the usual synchrotron formulae (e.g., Pacholczyk 1970) to solve for the equipartition field strength (eq. [A6]). Actually, the value of the average magnetic field for equipartition is inversely proportional to δ, so in practice, we need only calculate B'_{eq} for $\delta = 1$.

We then derive the expression for the IC emission (eq. [A11]) using the effective energy density of the CMB as seen by the jet fluid (eq. [A13]). We evaluate the quantity R (the ratio of IC to synchrotron luminosities) in two ways: First, we compute R from the integrated IC energy flux to the integrated synchrotron energy flux (eq. [A21]). This is done by converting observed synchrotron frequencies to electron energies (which involves the magnetic field strength) and integrating the IC emission from the same segment of the electron spectrum, taking into account the anisotropic radiation pattern of the IC component. Second, we compute the expected value of R from the ratio of the energy densities of the CMB to that in the magnetic field (both in the jet frame; eq. [A22]). Equating these two expressions, we are able to solve for the beaming parameters that satisfy the equality (eq. [A23]). Since the jet parameters enter the R equations in rather complex ways because of the anisotropic nature of the IC emission, a numerical method is used. This is demonstrated in Figure 1, and we obtain a result consistent with that of Celotti et al. (2001) for PKS 0637.

We use the following notation: we prime all quantities in the jet frame and, in cases where ambiguities could arise, we characterize jet parameters by the subscript j and electron parameters by the subscript e.

4.3. *Assumptions*

1. We assume that all the energy density of the CMB occurs at ν_{peak}, the peak of the blackbody distribution.

2. We assume that in the jet frame equipartition holds between the energy densities of the relativistic particles and the magnetic field. This allows us to estimate the average field strength in the source. Moreover, we take the volume filling factor to be 1 and the contribution to the particle energy density by protons to be nil. If relativistic protons contribute significantly to the particle energy density, B_{eq} increases and beaming parameters become more extreme (larger values of Γ and smaller angles).

3. The spectral index measured for the synchrotron spectrum at the lowest available frequencies continues unchanged to frequencies much lower that those accessible to Earth-based telescopes. The gross attributes of this

extrapolation must be consistent with radio emission arising from $\gamma'_e \approx 2000$ and X-ray emission (0.2–10 keV) arising from $25 < \gamma'_e < 300$. This extrapolation of the electron spectrum provides a large uncertainty in the beaming model and has been tacitly ignored by most previous formulations. At our current level of understanding, we do not have any convincing evidence on the amplitude or the power-law index of the electron distribution at low energies.

4.4. *Beaming Parameters for a Number of Sources*

In this section, we provide some of the key synchrotron parameters and beaming descriptors for a few knots in radio jets. For the synchrotron parameters, we use the standard expressions (e.g., Pacholczyk 1970) with observables transformed back to the jet frame. For the beaming parameters, our solution to equation (A23) requires only four numbers:

1. $B(1)$, the equipartition field from the synchrotron model when $\delta = 1$ (no beaming);
2. $R(1)$, the ratio of amplitudes of the power-law spectra, $k_{\rm IC}/k_{\rm sync}$, where both amplitudes must refer to the same spectral index;
3. z, the redshift; and
4. α, the spectral index.

Table 2 gives the results, and it can be seen that the beaming parameters range from quite modest values (e.g., PKS 1127) to rather unbelievable extremes (3C 120). We have plotted the key results in Figure 2, which is a representation of the beaming parameters as a function of the observables (eq. [A24]).

5. EVALUATION OF BEAMING AND SYNCHROTRON MODELS

In this section, we deal with the conflicting evidence for general beaming models and for synchrotron models. On the one hand, some sort of beaming appears to be required by the observation that all of the known jet sources (excluding, of course, the SSC terminal hot spots) produce X-ray emission on only one side, and that is the side which has the only or dominant radio jet and for which relativistic effects have been demonstrated (usually on VLBI scales). On the other hand, for knots such as A1/3C 273 or B/3C 390.3, the observed X-ray intensity is accommodated by an extension of the power law connecting the radio and optical (i.e., the synchrotron spectrum). If the X-ray emission from these knots were to be IC/CMB emission enhanced by beaming, this situation would be only a coincidence.

5.1. *X-Ray Spectra*

In general, we expect synchrotron spectra to be concave downward when plotted on the usual log S versus log ν plane. For high-energy electrons, this is caused by the E^2 losses. Although we do not have reliable observational evidence on the shape or amplitude of the electron spectrum for $\gamma \leq 500$, our expectation is that the spectrum observed in the radio regime might flatten at lower frequencies, but it is unlikely to steepen. This view is dictated by the requirement to avoid divergences in the total number of electrons and integrated energy in the electron spectrum.

Reliable X-ray spectra are now available for only a few jets, but so far, the evidence is that the spectra are either the same as observed in the radio/optical (e.g., 3C 273/A1; Marshall et al. 2001a) or steeper [α_x(M87) = 1.5 ± 0.4 (Böhringer et al. 2001) and α_x(3C 66B) ≈ 1.3 (Hardcastle et al. 2001b)]. This supports the synchrotron model and is not in accord with our expectation for beaming from low-energy electrons. However, a relatively hard spectrum is found for PKS 1127 ($\alpha_x = 0.5 \pm 0.2$; Siemiginowska et al. 2002), a jet that requires very modest beaming parameters. Similarly, Chartas et al. (2000) find $\alpha_x = 0.85 \pm 0.1$ for the outer jet in PKS 0637, another likely beamed IC source. The X-ray spectral index may prove to be a key parameter in differentiating synchrotron from beaming sources. The condition $\alpha_x \leq \alpha_r$ may be indicative of beaming, whereas $\alpha_x > \alpha_r$ is the condition we expect from homogeneous synchrotron models.

5.2. *Distinct Spectral Components*

By this we mean a population of relativistic electrons that is distinct from that which we measure in the radio/optical regime. The emitting volume could be quasi-coincident with that of the known synchrotron component, or it could be embedded within the known volume. For synchrotron models, a small, flat spectrum component is required. In the case of the 25″ knot in 3C 120, the current optical upper limits demand that $\alpha \leq 0.4$. A small region within the radio knot would be an efficient method to produce the observed X-rays in the sense that the total energy of such an entity would be very modest (Harris et al. 1998). As noted in § 5.1, the spectral data so far available do not support this sort of scenario.

For the IC/CMB model without beaming, what is required is an excess population of electrons with γ in the range 500–2000. For bulk relativistic velocities, this energy range shifts to lower values since the peak of the CMB appears blueshifted to the jet.

5.3. *Jet Length and Structure*

The beaming model has untenable consequences for straight jets. In general, the angle, θ, between the jet axis and line of sight to the observer derived for jets such as 3C 273 is not very different from those found at VLBI scales, and this jet appears straight on the kiloparsec scale. If the jet fluid moves in a straight line along the axis of the jet, then the physical length of the jet is the projected length divided by sin θ. In Table 2 we have listed these values, which range up to a megaparsec for 3C 273. Very few radio sources are directly observed (i.e., in the plane of the sky) to have such large physical sizes.

These excessive lengths can be avoided in at least two ways. We know that some jets bend (e.g., 3C 120). If the apparently straight jets (e.g., 3C 273) were to bend significantly in a plane normal to the plane of the sky, they would appear straight, but the beaming required for a particular feature would not apply to the whole jet. The other possibility is that the jet fluid responsible for the observed radiation would not be constrained to move along the jet axis but, for example, might follow a helical path (see, e.g., Meier, Koida, & Uchida 2001) around the axis as suggested by the *Hubble Space Telescope* (*HST*) images of 3C 273, or the emission regions might represent all or a portion of the flow being deflected toward the observer.

Whichever of these possibilities might be operative, it should work in conjunction with the requirement that the jet seen is the one approaching the observer.

5.4. *Evidence for Bulk Relativistic Velocities and Cold Jets*

Are there reasonable expectations for kiloparsec-scale relativistic velocities aside from their utility in explaining X-ray emission? Bridle (1996) marshals considerable evidence for bulk relativistic velocities at least for the inner section of FR I jets and all the way out to the terminal hot spots for FR II radio galaxies and quasars. Although representative values for such velocities are not presented, we infer Γ-values of at least a few. Wardle & Aaron (1997), while agreeing that one-sidedness evidence supports relativistic velocities in jets, argue that the observed dispersion in the ratio of the flux density of the inner straight part of the jet (the feature expected to be most enhanced by beaming) to the flux density of the lobe (no beaming) is less than the expected dispersion for $\Gamma \approx 5$. Thus, they conclude that the characteristic jet speed is $\beta \approx 0.85$ ($\Gamma \approx 2$) and that all jets decelerate between parsec and kiloparsec scales.

The consideration of large Γ-values for kiloparsec-scale jets reminds us of the problem of energy transport. If electrons were to be a significant component of the jet, they could not escape the IC losses, which increase as Γ^2. Since these losses go as γ^2, we may expect that only low-energy electrons survive for long distances. Thus, the energy must be transported by Poynting flux, protons, or cold electrons and positrons. If the latter, it might be possible to explain the relatively smooth X-ray emission, such as that underlying the 3C 273 knots or the Pictor A inner jet, as IC beamed emission from essentially cold electrons that are characterized by $\Gamma \geq \gamma$. The brighter knots would then rely on the conventional shock acceleration and/or pair production to generate (in situ) the usual power-law distribution of relativistic electrons with γ-values of normal synchrotron sources.

5.5. *Offsets between Radio and X-Ray–Brightness Peaks*

The synchrotron expectation is that lower frequency emission will persist further downstream since the higher energy electrons have shorter lifetimes. However, at the site of the shock, there should be strong emission at all frequencies (e.g., M87, knot A). In the beaming model, one way to accommodate a leading X-ray feature is to argue for the existence of a precursor shock that is incapable of producing electrons with $\gamma \geq 1000$.

5.6. *Progression of Brightnesses for Multiple-Knot Jets*

In the optical, the 3C 273 jet has a series of well-defined knots with comparable brightnesses and fluxes. However, at radio wavelengths, the knot intensities increase going out of the jet, and the situation is reversed for X-rays. This X-ray and radio behavior is mimicked in PKS 1127. As a natural consequence, the parameters for the beaming model become less restrictive (smaller Γ, larger θ) as the distance from the core increases.

This sort of behavior is consistent with synchrotron models for which we might well expect that the properties of shocks that permit them to produce copious supplies of the highest energy electrons will diminish as we move out to larger distances.

5.7. *Is Overproduction a Problem?*

The beaming model means that the underlying synchrotron components are significantly less energetic than for the stationery synchrotron model. Typical luminosities drop from 10^{41} ergs s^{-1} to values like 10^{38} ergs s^{-1}. Such entities must be very common in jets, so might we expect to be overwhelmed with X-ray emission from excessive numbers of weak synchrotron emitters that happen to be moving toward us?

6. CONCLUSIONS

There is little doubt in our minds that thermal bremsstrahlung is not a major contributor to the X-ray emission from most of the jet features discussed in this paper. We find the arguments in favor of SSC emission from terminal hot spots of a few FR II radio galaxies to be convincing.

The failure of simple synchrotron models to fit the spectra of some features, together with the quasi universality of one-sidedness, almost demands the occurrence of relativistic bulk velocities. On the other hand, extreme values for the beaming parameters together with the excellent agreement of the X-ray spectra with the extrapolation of the radio-optical spectra for many features lend strong support to the synchrotron models.

Thus, the leading contender for most of the X-ray jets appears to be a single or multiple spectral component synchrotron model augmented by a modest beaming with $\Gamma < 10$ to account for the one-sidedness of most of the recorded X-ray features. The IC/beaming hypothesis can consistently explain the emission from several jets, and the low required beaming factors for some sources (e.g., PKS 1127) make it probable that this emission component contributes substantially to the observed X-ray fluxes of at least some of the observed X-ray features. Higher redshifts and steeper radio spectra appear to favor beaming, while local sources with flatter radio spectra are probably dominated by synchrotron emission.

D. E. H. thanks W. Tucker for extensive discussions during the early phases of this investigation, T. Kneiske for discussions on comparison of beaming formulations, and A. Bridle for discussing the radio aspects of jets. We also thank M. Hardcastle, M. Birkinshaw, and R. Sambruna for communicating results prior to publication and A. Siemiginowska and H. Marshall for sharing their proprietary data. M. Birkinshaw, D. Worrall, W. Forman, F. Aharonian, and A. Marscher provided helpful suggestions for improving the manuscript, and the anonymous referee supplied useful criticisms. H. K. thanks P. Coppi for discussions on active galactic nucleus jets and acknowledges support by NASA (NAS8-39073 and GO 0-1169X). The work at SAO was partially supported by NASA contract NAS8-39073.

APPENDIX A

FORMULATION OF BULK RELATIVISTIC BEAMING WITH EQUIPARTITION FIELDS

We first find the synchrotron parameters in the jet frame and then derive expressions for the IC emission. Then we obtain two expressions for the ratio of IC to synchrotron losses: one based on the observed data and one based on the energy densities of photons and magnetic fields. Equating these two expressions provides the final beaming equation. We use cgs units throughout except where stated otherwise.

The basic relationships for the parameters that describe the bulk motion of the jet fluid are the jet velocity, $\beta_j \equiv v/c$, the Lorentz factor, Γ, the angle of the fluid's velocity with respect to the line of sight of the observer, θ_j, and the Doppler beaming factor, δ:

$$\Gamma \equiv \frac{1}{\sqrt{1-\beta^2}}\,, \tag{A1}$$

$$\delta^{-1} \equiv \Gamma(1-\beta\cos\theta)\,. \tag{A2}$$

A1. THE SYNCHROTRON PARAMETERS IN THE JET FRAME

The required observables are

1. the size of the emitting volume;
2. α, the low-frequency spectral index of the synchrotron spectrum;
3. ν_1 and ν_2, the lower and upper limits of the synchrotron spectrum in the observer frame (N.B., it may be necessary to decrease ν_1 to ≈ 1 MHz so as to include low-γ electrons required for the beaming model);
4. S_0 at some ν_0, with S_0 the flux density observed at the Earth and ν_0 the frequency at the receiver corresponding to S_0; this provides k_s, the amplitude of the observed synchrotron spectrum: $k_s = S_0\,\nu_0^{\alpha}$; and
5. the luminosity distance and redshift.

We then move to the jet frame. Frequencies convert as

$$\nu' = \nu(1+z)/\delta\,. \tag{A3}$$

Assuming a knotty jet and neglecting complications arising from different pattern and jet plasma velocities, we find from the Lorentz invariant, S/ν^3 (see also eqs. [C7] and [C11] of Begelman, Blandford, & Rees 1984), the monochromatic luminosity per solid angle in the jet frame:

$$l'_{\Omega',\nu'} = \frac{k_s(\mathrm{obs})\nu'^{-\alpha}(1+z)^{\alpha-1}D_L^2}{\delta^{3+\alpha}}\ \mathrm{ergs\ s^{-1}\ Hz^{-1}\ sr^{-1}}\,. \tag{A4}$$

Here, D_L is the luminosity distance and $(1+z)^{\alpha-1}$ is the K-correction. This equation allows evaluation of $l'_{\Omega',\nu'}$ at any convenient frequency in the jet frame. Integrating over frequency and solid angle, the total luminosity becomes

$$L'_s = \frac{4\pi D_L^2}{\delta^4}\left[\frac{k_s(\nu_2^{1-\alpha}-\nu_1^{1-\alpha})}{1-\alpha}\right] = \frac{L_s}{\delta^4}\ \mathrm{ergs\ s^{-1}}\,. \tag{A5}$$

The right term is the energy flux at the Earth, $4\pi D_L^2$ computes the luminosity at the source, and δ^4 transforms into the jet frame.

To compute the equipartition magnetic field in the jet frame (e.g., eq. [7.12] of Pacholczyk 1970),

$$B'_{\mathrm{eq}} = \left[\frac{18.85C_{12}(1+k)L'_s}{\phi V'}\right]^{2/7}\ \mathrm{G}\,. \tag{A6}$$

V′ is the emitting volume; ϕ is the volume filling factor; and C_{12} is a Pacholczyk parameter that is a slowly varying function of α, ν'_1, and ν'_2 (e.g., $C_{12} = 5.7\times 10^6$ for $\alpha = 0.8$, $\nu'_1 = 10^7$, and $\nu'_2 = 10^{15}$). When the correct expression for C_{12} is used in equation (A6), it introduces an extra factor of $\delta^{0.5}$ to the numerator within square brackets, so that together with the explicit δ^4 from equation (A5), which appears in the denominator, the final dependency within the square brackets goes as $\delta^{-7/2}$, and hence

$$B'_{\mathrm{eq}} = \frac{B(1)}{\delta}\,, \tag{A7}$$

where $B(1)$ is the equipartition field calculated for no beaming ($\delta = 1$).

A2. CONVERTING ANGLES TO THE JET FRAME IN ORDER TO CALCULATE THE INVERSE COMPTON EMISSION

From manipulation of the basic equations (A1) and (A2),

$$\mu_j \equiv \cos(\theta_j) = \frac{\Gamma - 1/\delta}{\sqrt{\Gamma^2-1}}\,. \tag{A8}$$

Since in the jet frame most of the CMB photons will come from the direction in which the jet plasma is moving and the scattered IC emission from a particular electron will be strongly beamed into the direction of the instantaneous velocity vector of the electron, the IC emission will not be isotropic in the jet frame. Take the angle between the line of sight to the observer and the jet axis as θ_j and θ'_j in the observer and jet frames, respectively. Likewise, μ_j and μ'_j are the corresponding cosines. Then,

$$\mu'_j = \frac{\mu_j - \beta_j}{1 - \mu_j \beta_j} , \tag{A9}$$

where β_j is the velocity of the jet (see, e.g., Pacholczyk 1970, eq. [5.25]). The inverse is also useful:

$$\mu_j = \frac{\mu'_j + \beta_j}{1 + \mu'_j \beta_j} . \tag{A10}$$

To calculate the power emitted by an electron traveling at an angle Θ' to the seed photon direction, we use $\Theta' \approx \theta'_j$ and follow Rybicki & Lightman (1979, p. 199; see also Dermer, Schlickeiser, & Mastichiadis 1992) to get

$$\frac{dE'}{dt} = c\sigma_{\rm T} u'_{\rm CMB} \kappa \text{ ergs s}^{-1} , \tag{A11}$$

$$\kappa = \gamma'^2_e(1 + \beta'_e \mu'_j)^2 - (1 + \beta'_e \mu'_j) , \tag{A12}$$

where $\sigma_{\rm T}$ is the Thomson cross section, E' is the energy of the electron, $u'_{\rm CMB}$ is the Doppler-boosted energy density of the CMB, and γ'_e, β'_e are the Lorentz factor and velocity of the electron in the jet frame.

The second term in equation (A12) will be negligible except when μ'_j approaches -1, which is the case for electrons moving directly away from the jet's velocity vector.

The energy density of the CMB (as seen by the jet moving with Γ) is

$$u'_{\rm CMB} = 4 \times 10^{-13}(1 + z)^4(4/3)(\Gamma^2 - 1/4) \text{ ergs cm}^{-3} . \tag{A13}$$

The peak frequency of the CMB (again, as seen by the jet) is

$$\nu'_p = 1.6 \times 10^{11}(1 + z)\Gamma \text{ Hz} . \tag{A14}$$

In the jet frame, the mean energy of photons scattered in the direction θ'_j will be

$$\langle \varepsilon'_{\rm IC} \rangle = \frac{dE'/dt'}{c\sigma_{\rm T} n'_{\rm CMB}(1 + \beta'_e \mu'_j)} \text{ ergs} \tag{A15}$$

$$= \frac{\langle \varepsilon'_p \rangle \kappa}{1 + \beta'_e \mu'_j} \text{ ergs} \tag{A16}$$

$$= \langle \varepsilon'_p \rangle [\gamma'^2_e(1 + \beta'_e \mu'_j) - 1] \text{ ergs}, \tag{A17}$$

where $\langle \varepsilon'_p \rangle$ is the mean energy of the photons before scattering, $1.6 \times 10^{11}(1 + z)\Gamma$, and $n'_{\rm CMB}$ is the seed photon density in the jet frame, so that the denominator in equation (A15) is the (expected) number of scatterings per unit time for one electron.

A3. THE EXPRESSION FOR THE OBSERVED RATIO OF LUMINOSITIES, R(obs)

We define R as the ratio of IC and synchrotron luminosities. Since both of these losses go as the electron energy squared, all electrons will experience the same value of R.

For $\alpha = 1$ there is equal energy per decade, and thus the integration band is not important, so that the ratio of luminosities is equal to the ratio of amplitudes of the X-ray (IC) and radio (sync) spectra,

$$R(1) = \frac{L_{\rm IC}}{L_{\rm sync}} = \frac{k_x}{k_r} . \tag{A18}$$

For $\alpha \neq 1.0$, to obtain $L_{\rm IC}/L_{\rm sync}$ we change integration parameters from ν' to γ'. These conversions are found by using equation (A17) with $\beta'_e = 1$ and dropping the -1:

$$\nu'_{\rm IC} = (1 + \mu'_j)\gamma'^2_e[1.6 \times 10^{11}(1 + z)\Gamma] \text{ Hz} \tag{A19}$$

(the last term is the peak frequency of the CMB in the jet frame),

$$\nu'_{\rm sync} = 4.202 \times 10^6 \gamma'^2_e \times B' \text{ Hz}. \tag{A20}$$

Then most of the factors of equation (A5), including the integration itself, cancel, and the remaining parameters are those resulting from the different conversions of ν to γ. After these manipulations, we find

$$R(\text{obs}) = R(1)\left[\frac{3.808 \times 10^4(1+z)(1+\mu'_j)\Gamma}{B'_{\text{eq}}}\right]^{1-\alpha} . \tag{A21}$$

A4. EVALUATE R FROM RATIO OF ENERGY DENSITIES, R(exp)

The ratio of the IC and synchrotron luminosities can be computed from the ratio of energy densities in photons and magnetic field. This provides an expression for the "expected" value of R. In using equation (A12), we have dropped the second term since it will normally be much smaller than the first term:

$$R(\text{exp}) = \frac{U'_{\text{CMB}}}{u'(B'_{\text{eq}})} = \frac{4 \times 10^{-13}(1+z)^4(1+\mu'_j)^2[\Gamma^2 - (1/4)]}{B'^2_{\text{eq}}/8\pi} , \tag{A22}$$

where U'_{CMB} is the CMB energy density in the jet frame, modified by the deviation from the beamed emission power from that computed for an isotropic seed photon field.

A5. THE BEAMING EQUATION

Equating the two expressions for R (eqs. [A21] and [A22]),

$$\Gamma^{\alpha+1} - \frac{\Gamma^{\alpha-1}}{4} = R(1)\,\frac{9.947 \times 10^{10}(3.808 \times 10^4)^{1-\alpha}}{(1+z)^{3+\alpha}}\left(\frac{B'_{\text{eq}}}{1+\mu'_j}\right)^{\alpha+1} . \tag{A23}$$

Thus, with four parameters that depend on the observable data [α, z, $B(1)$, and $R(1)$] we can solve equation (A23) numerically by finding the range of μ' and Γ pairs that satisfy the equation.

If we ignore the second Γ term and replace B' with equation (A7), we obtain an approximate expression for the beaming parameters in terms of the observables (see Fig. 2):

$$\Gamma\delta(1+\mu'_j) = \frac{B(1)[10^{11}R(1)]^{1/(1+\alpha)}(3.808 \times 10^4)^{(1-\alpha)/(1+\alpha)}}{(1+z)^{(\alpha+3)/(\alpha+1)}} . \tag{A24}$$

APPENDIX B

FREQUENCIES, ELECTRON ENERGIES, AND HALF-LIVES

Once we have the allowed values of θ_j, δ, and Γ, we need to determine where the emission bands occur and which segments of the electron energy spectrum are responsible for the observed radiation.

To determine the IC emission frequency of electrons responsible for a particular synchrotron frequency,

$$\nu_{\text{IC}}(\text{obs}) = \nu_s(\text{obs})3.808 \times 10^4(1+\mu'_j)\Gamma(1+z)/B' \text{ Hz} , \tag{B1}$$

and the reverse,

$$\nu_s(\text{obs}) = \frac{\nu_{\text{IC}}(\text{obs})2.626 \times 10^{-5}B'}{\Gamma(1+z)(1+\mu'_j)} \text{ Hz} . \tag{B2}$$

To find the electron energy responsible for a particular synchrotron frequency, we use equations (A3), (A7), and (A20):

$$\gamma'^2_e = \frac{2.380 \times 10^{-7}\nu_s(\text{obs})(1+z)}{B'\delta} . \tag{B3}$$

For the electron energy responsible for an IC frequency, we use equations (A3) and (A19):

$$\gamma'^2_e = \frac{6.25 \times 10^{-12}\nu_{\text{IC}}(\text{obs})}{(1+\mu'_j)\delta\Gamma} . \tag{B4}$$

For the half-lives, we use the normal expression: $(dE/dt) \times \tau = E/2$. This results in

$$\tau' = \frac{10^{13}}{\gamma'_e\{1.016B'^2 + 10.398(1+z)^4[\Gamma^2 - (1/4)][(1+\beta'_e\mu'_j)^2 - (1+\beta'_e\mu'_j)/\gamma'^2_e]\}}, \tag{B5}$$

where B' is in μG and τ' is in years.

Making the usual approximations for quantities close to 1 and since time intervals in the jet frame are observed at the Earth as

$$\tau_0 = \tau' \frac{1+z}{\delta}, \tag{B6}$$

an approximate expression for the observed half-life is

$$\tau_0 = \frac{10^{13}(1+z)}{\gamma'_e\,\delta[B'^2 + 40(1+z)^4\Gamma^2]}\ \text{yr}. \tag{B7}$$

REFERENCES

Aharonian, F. A. 2001, MNRAS, in press (astro-ph/0106037)
Begelman, M., Blandford, R., & Rees, M. 1984, Rev. Mod. Phys., 56, 255
Biretta, J. A., Stern, C. P., & Harris, D. E. 1991, AJ, 101, 1632
Bodo, G., Ghisellini, G., & Trussoni, E. 1992, MNRAS, 255, 694
Böhringer, H., et al. 2001, A&A, 365, L181
Bridle, A. H. 1996, in ASP Conf. Ser. 100, Energy Transport in Radio Galaxies and Quasars, ed. P. E. Hardee, A. H. Bridle, & J. A. Zensus (San Francisco: ASP), 383
Brunetti, G., Cappi, M., Setti, G., Feretti, L., & Harris, D. E. 2001, A&A, 372, 755
Burbidge, G. R. 1956, ApJ, 124, 416
Carilli, C. L., Perley, R. A., & Harris, D. E. 1994, MNRAS, 270, 173
Celotti, A., Ghisellini, G., & Chiaberge, M. 2001, MNRAS, 321, L1
Chartas, G., et al. 2000, ApJ, 542, 655
Dermer, C. D., Schlickeiser, R., & Mastichiadis, A. 1992, A&A, 256, L27
Ginzburg, V. L., & Syrovatskii, S. I. 1969, ARA&A, 7, 375
Hardcastle, M. J., Birkinshaw, M., & Worrall, D. M. 2001a, MNRAS, 323, L17
———. 2001b, MNRAS, 326, 1499
Harris, D. E., Carilli, C. L., & Perley, R. A. 1994, Nature, 367, 713
Harris, D. E., et al. 2000, ApJ, 530, L81
Harris, D. E., Hjorth, J., Sadun, A. C., Silverman, J. D., & Vestergaard, M. 1999, ApJ, 518, 213
Harris, D. E., Leighly, K. M., & Leahy, J. P. 1998, ApJ, 499, L149
Kraft, R. P., et al. 2000, ApJ, 531, L9
Mannheim, K., Krulls, W. M., & Biermann, P. L. 1991, A&A, 251, 723
Marshall, H., et al. 2001a, ApJ, 549, L167
———. 2001b, ApJ, submitted
Meier, D. L., Koide, S., & Uchida, Y. 2001, Science, 291, 84
Pacholczyk, A. G. 1970, Radio Astrophysics (San Francisco: Freeman)
Readhead, A. C. S. 1994, ApJ, 426, 51
Rybicki, G. B., & Lightman, A. P. 1979, Radiative Processes in Astrophysics (New York: Wiley)
Sambruna, R. M., Urry, C. M., Tavecchio, F., Maraschi, L., Scarpa, R., Chartas, G., & Muxlow, T. 2001, ApJ, 549, L161
Schreier, E. J., Gorenstein, P., & Feigelson, E. D. 1982, ApJ, 261, 42
Siemiginowska, A. L., et al. 2002, ApJ, submitted
Singal, A. K. 1986, A&A, 155, 242
Tavecchio, F., Maraschi, L., Sambruna, R. M., & Urry, C. M. 2000, ApJ, 544, L23
Wardle, J. F. C., & Aaron, S. E. 1997, MNRAS, 286, 425
Wilson, A. S., Young, A. J., & Shopbell, P. L. 2000, ApJ, 544, L27
———. 2001, ApJ, 547, 740